EPJ Web of Conferences **282**, 01009 (2023) https://doi.org/10.1051/epjconf/202328201009
SSP 2022

Observation of the $\gamma\gamma \rightarrow \tau\tau$ process in Pb+Pb collisions and constraints on the τ-lepton anomalous magnetic moment with the ATLAS detector at LHC

Vincenzo Cavasinni[1]
on behalf of the ATLAS Collaboration

[1]Dipartimento di Fisica "E.Fermi" dell'Università and INFN Pisa

Abstract. This paper reports the observation of τ-lepton pair production in ultraperipheral lead-lead collisions, $Pb(\gamma)Pb(\gamma) \rightarrow \tau\tau$ and constraints on the τ-lepton anomalous magnetic moment, a_τ, measured by the ATLAS experiment. The dataset corresponds to an integrated luminosity of 1.44 nb^{-1} of LHC Pb+Pb collisions at $\sqrt{s_{NN}}$=5.02 TeV. Selected events contain one muon from a τ-lepton decay, an electron or charged-particle track(s) from the other τ-lepton decay, little additional central-detector activity, and no forward neutrons. The $\gamma\gamma \rightarrow \tau\tau$ process is observed in Pb+Pb collisions with a signal strength of $\mu_{\tau\tau}= 1.03\ ^{+0.06}_{-0.05}$. To measure a_τ, a template fit to the muon transverse-momentum distribution from τ-lepton candidates is performed, using a dimuon ($\gamma\gamma \rightarrow \mu\mu$) control sample to constrain systematic uncertainties. The observed 95% confidence-level interval for a_τ is $(-0.057, 0.024)$.

1 Introduction

The magnetic moment μ_B is proportional to the particle spin through the parameter g: $\mu_B = g\frac{e\hbar}{2m}$. In the Dirac theory $g = 2$ and the anomalous magnetic moment a is defined as $a = \frac{g-2}{2}$. The first QED correction to Dirac theory for electrons was calculated by J. Schwinger in 1948: $a_e = \alpha/2\pi = 0.00116$ [1]. In the Standard Model (SM) higher order corrections predict a to be of the order of 10^{-3} calculated with high precision that requires to be verified with corresponding accurate measurements. Discrepancies between the SM predictions and the measurements would suggest new physics beyond SM, eg: lepton- compositeness, supersymmetric particle, ...

For electrons and muons the measurements of a have been performed with a precision of 0.28 ppb [2] and 0.46 ppm [3] with differences from SM predictions of 2.4 and 4.6 standard deviations, respectively. Therefore the precise measurements of the lepton anomalous moment represent one of the most powerful tools to check the validity of the SM in searching for new physics.

For a_τ, at the present, the experimental measurement is much less precise than those possible for the other two charged leptons. On the other hand, theoretically, the larger $\tau-$mass enhances the contributions to a from new particles of mass M; in fact the photon-lepton vertex coupling is expected to be of the order of m_l^2/M^2 for a lepton of mass m_l. Therefore new physics effects for τ's would be larger by a factor $m_\tau^2/m_\mu^2 = 286$ compared with the case of muons. The present experimental knowledge of a_τ is quite poor: the very short τ-lifetime

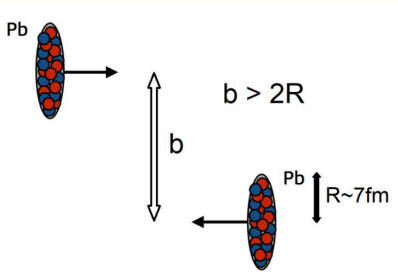

Figure 1. Example of Pb-Pb ultraperipheral collision. Pb-Pb collisions occurring at an impact parameter b large, say twice the Pb nucleus radius, are not affected by strong nucleon-nucleon interactions and they are called Ultra Peripheral Collisions.

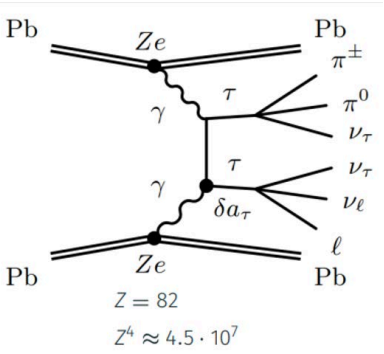

Figure 2. Diagram of pair-production of tau leptons from ultraperipheral Pb-ion collisions. One τ decays into μ + neutrinos, the other τ decays into 3 pions + neutrino. New physics modifies the magnetic moment by δa_τ.

precludes the use of the precession frequency measurement method as done in the $\mu-$case. The method adopted was then to measure the $\tau - pair$ production cross-section, total and differential, in photon-photon scattering, where these quantities are sensitive to a_τ. The best a_τ measurement was obtained by the DELPHI experiment at LEP [4]:$-0.052 < a_\tau^{exp} < 0.013$ at 95% CL, or, expressed as a central value and an error, $a_\tau^{exp} = -0.018(17)$.

The theoretical SM expectation for a_τ , which includes electroweak and hadronic contributions, is calculated in [5]: $a_\tau^{SM} = 117721(5) \times 10^{-8}$ with a precision by far better than that of the experiments. So any effort should be made experimentally to approach in precision at least the size of the prediction of the SM: $a_\tau = 10^{-3}$.

The ATLAS experiment [6] has measured a_τ using Pb-Pb ultra peripheral collisions (UPC) at LHC to single-out $\gamma - \gamma$ collisions yielding tau-pairs. This reaction has several advantages compared with other reactions at LHC. In fact in UPC Pb-Pb collisions, Figure 1, the τ-pairs are generated by a $\gamma\gamma$ collision [1], Figure 2. The cross-section is strongly enhanced by a factor Z^4, largely compensating the lower luminosity compared with that available in proton-proton collisions. In addition, the request of the presence of only the tau-decay products in the detector, with essentially no pile-up background, makes the control of backgrounds (electron/muon/quark pairs) much easier than in case of p-p collisions.

2 The analysis strategy

This paper presents the observation of the $Pb(\gamma)Pb(\gamma)) \rightarrow \tau\tau$ process and measurement of a_τ [6] using 1.44 nb^{-1} integrated luminosity at $\sqrt{s_{NN}} = 5.02$ TeV Pb+Pb data recorded by ATLAS in 2018.

The a_τ measurement in ATLAS is performed by looking at the dependence of the $Pb(\gamma)Pb(\gamma) \rightarrow \tau\tau$ cross-section and τ-p_{T} distribution. Figure 3 [7] shows the a_τ dependences of cross-section, left plot, and of τ-p_{T} distribution, central and right plots, for negative and positive a_τ, respectively.

[1]The first idea of using photons accompanying fast moving charged particles for physics experiments is due to Enrico Fermi in 1924 [8].

The ATLAS detector [9] is a multipurpose particle detector with cylindrical geometry, comprising an inner detector (ID) tracker, electromagnetic (EM), hadronic calorimeters and a muon spectrometer (MS). The zero-degree calorimeters (ZDC) [10] are located at $z = 140$ m in both sides from the interaction point and detect neutral particles such as neutrons emitted from interacting nuclei.

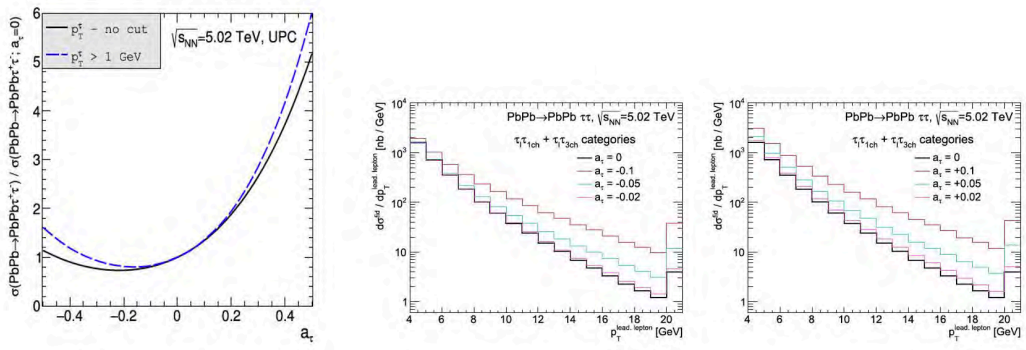

Figure 3. τ-pair cross-section dependence on a_τ (normalised to $a_\tau = 0$) (left), and τ-p_{T} distribution as a function of positive (central) and negative (right) a_τ[7].

After the UPC Pb-Pb interaction, the ions can remain intact, enabling selection of low-multiplicity events with one muon originating from one of the τ-leptons, while the other τ-lepton decay is reconstructed as either an electron or one or three charged-particle tracks with low transverse momentum. The trigger required one muon with $p_{\mathrm{T}} > 4$ GeV, low activity in the forward calorimeters and no neutron in the very forward calorimeter ZDC.

Samples of simulated $\gamma\gamma \to \tau\tau$ signal events were produced at leading order in QED using the Starlight 2.0 [11] Monte Carlo (MC) generator for lepton-pair production in UPC events, interfaced with Tauola [12] for τ-lepton decays. The dominant background sources is the $\gamma\gamma \to \mu\mu$ process, its contribution is estimated with the aid of MC samples generated using Starlight; Pythia 8 was used to model EM FSR from the muons.

Selected events must contain one muon, which targets a muonic decay of one of the τ leptons. Three signal regions (SR) then categorise events by the decay signature of the other τ-lepton. The μe-SR category additionally requires one electron, and no additional tracks which targets fully leptonic decays of both τ-leptons. The $\mu 1T$-SR ($\mu 3T$-SR) category requires exactly one track (three tracks) separated from the muon by $\Delta R(\mu - trk) > 0.1$ [2], which targets τ-lepton decays to one or three charged hadrons. The one-track requirement also captures leptonic τ-lepton decays that fail electron or muon reconstruction. The electric charges of muon, electron, and tracks must sum to zero. Figure 4 shows the display of a candidate signal event in $\mu 3T$-SR.

To constrain the $\gamma\gamma \to \mu\mu$ a control region (CR) of dimuon events called 2μ-CR is defined. It requires exactly two muons with invariant mass above 11 GeV to suppress quarkonia ($Y_{nS} \to \mu\mu$) backgrounds and no additional tracks separated from the muons by $\Delta R(\mu - trk) > 0.1$. The 2μ-CR sample was used also to constrain the systematic uncertainty arising from the knowledge of $\gamma\gamma$ flux.

[2] $\Delta R(\mu - trk) = \sqrt{(\eta_\mu - \eta_{trk})^2 + (\Phi_\mu - \Phi_{trk})^2}$ where η_μ, Φ_μ and η_{trk}, Φ_{trk} are the pseudorapidities and the azimuthal angles of the muon and of the track, respectively.

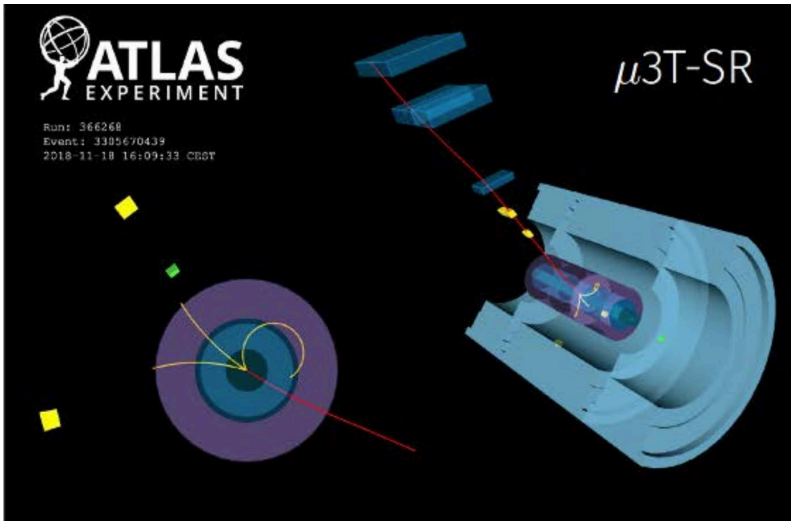

Figure 4. Display of a candidate event in the central ATLAS detector: a muon (red track) + 3 tracks. The muon is measured by the muon-spectrometer while the tracks are measured by the central ATLAS tracker [6].

The second most important background, significant only for μ1T-SR and μ3T-SR, comes from the diffractive photo-nuclear events where the Pb-ions may not dissociate failing the ZDC neutron veto. This background was estimated by a data-driven method using dedicated CRs called μ2T-CR and μ 4T-CR, which apply the same selection as μ1T-SR and μ3T-SR, but require an additional low energy track satisfying $p_T < 0.5$ GeV, relaxing the veto on unmatched clusters and extrapolating the number of events to zero unmatched clusters (the signal region) (see ref. [6] for details) .

Other sources of background are predicted to be negligible in the SRs. The uncertainty in the integrated luminosity is 1.9%, obtained using the LUCID-2 detector [13] for the primary luminosity measurements.

3 The prefit distributions

To verify the goodness of the Monte Carlo predictions compared to the data, the 2μ-CR events have been used. Figure 5 and Figure 6, show the leading muon p_{T}-distribution and the muon-pair invariant mass distributions in the 2μ-CR region. The data are compared to the predictions of STARLIGHT simulation improved at $p_T^{\mu} > 2GeV$ with events from the Madgraph Montecarlo which provides a better description of $\gamma\gamma \rightarrow \mu\mu(\gamma)$ processes. The agreement between prediction and data is fairly good, with a little contribution from non $\gamma\gamma \rightarrow \mu\mu$ events (including possible $\gamma\gamma \rightarrow \tau\tau$ events with both τ's decaying into muon + neutrinos).

Figure 7 shows for the 3 signal regions the prefit distributions of the muon-track p_T ($\mu 1T$-SR), left, 3track invariant mass distribution ($\mu 3T$-SR), central, and μe invariant mass distribution (μe-SR), right; Figure 7 shows the data compared to the signal and background contributions estimated with STARLIGHT+Madgraph Montecarlo and with a data-driven method for the $\mu\mu$ and photonuclear events, respectively.

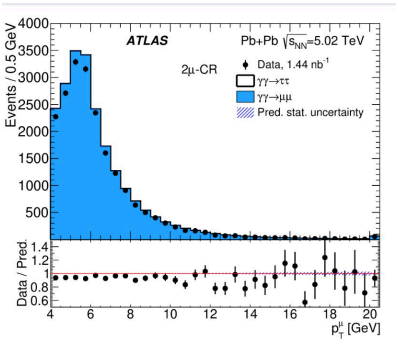

Figure 5. Leading muon p_T-distribution in 2μ-CR region [6].

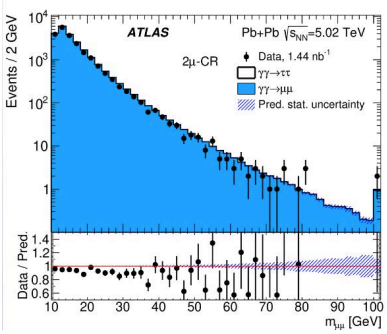

Figure 6. muon-muon invariant mass in 2μ-CR region [6].

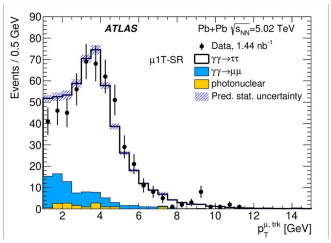

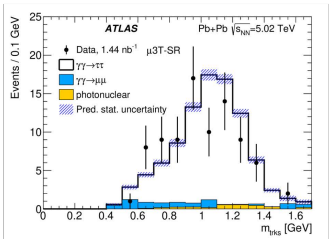

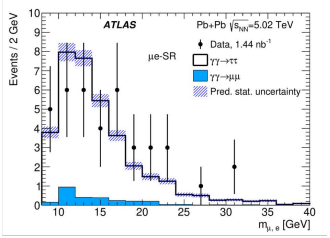

Figure 7. Signal region $\mu 1T$-SR: p_{T}-distribution of $\mu - track$ (left); Signal region $\mu 3T$-SR: 3-tracks invariant mass distribution (central); Signal region μe-SR: muon-electron invariant mass distribution (right) [6].

After applying the event selection, there are a total of 656 candidate events in the 3 signal regions with 80 and 16 estimated background events from $\mu\mu$ and photonuclear processes. The agreement between the predictions and the data is good for the three signal region plots.

4 Fitting the data

A profile likelihood fit to the muon-p_T distribution in the three SRs and 2μ-CR regions was used to extract the $\gamma\gamma \to \tau\tau$ signal strength: $\mu_{\tau\tau} = \frac{\sigma_{\tau\tau}^{data}}{\sigma_{\tau\tau}^{predicted}}$ and a_τ.

To measure a_τ, in particular, a fit is performed where a_τ is the only free parameter using the p_T^μ distribution in the three SRs and 2μ-CR; p_T^μ is chosen because of its high sensitivity to a_τ [7]. Simulated signal samples with various a_τ values are employed. In the nominal sample, a_τ is set to its SM value. Signal templates for alternative a_τ hypotheses, are obtained by modifying the $\gamma\tau\tau$ coupling in the Montecarlo-Lagrangian describing the process. Then the nominal sample is reweighted in three dimensions: differentially in $\tau\tau$ invariant mass, $\tau\tau$ rapidity, and rapidity difference between the two $\tau - leptons$, according to calculations from Ref. [7]. Note that the 3 kinematical parameters are sufficient to determine the p_T of the two τ's and, as a consequence, the p_T of the muon from the $\tau - decay$.

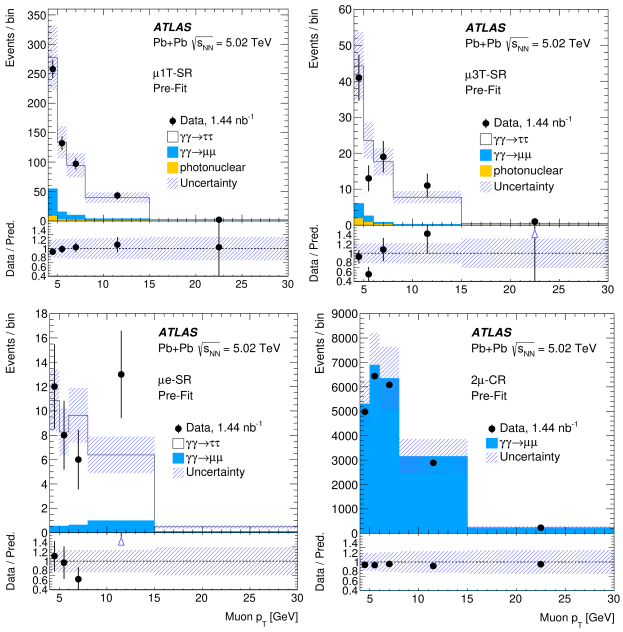

Figure 8. Prefit muon-p_T distributions for data and predictions, in the 3 signal regions and in the control region μ-CR. In the signal regions it is assumed the SM value of a_τ. Below each plot the ratio data/prediction is shown [6].

The main systematic uncertainties (in addition to the uncertainty in the photon flux) are: the muon-trigger efficiency, the muon/electron reconstruction/identification efficiency and calibration and the track reconstruction efficiency.

Figure 8 shows, for data and predictions, the muon-p_T distribution for the 3 signal regions and the control region 2μ-CR. The agreement between data and MC prediction is good; the largest systematic uncertainty in all distributions comes from the photon flux modelling which affects the signal yield by about 20%.

Figure 9 shows, for data and predictions, for the 3 signal regions and the control region 2μ-CR, the muon-p_T distributions. The results are obtained by a simultaneous fit using all regions. The inclusion of the 2μ-CR sample in the combined fit, strongly reduces the uncertainty originated by the photon flux modelling. The fit describes the data well. The evidence

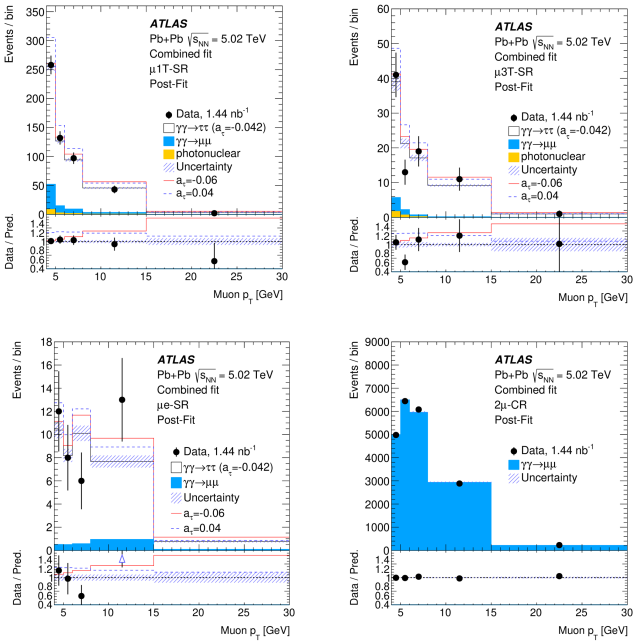

Figure 9. Muon p_T-distribution in μ1T-SR (top-left). Muon p_T-distribution in μ3T-SR (top-right). Muon p_T-distribution in μe-SR (bottom-left). Muon p_T-distribution in 2μ-CR (bottom-right). Black markers denote data and stacked histograms indicate the different components contributing to the regions. Post-fit distributions are shown with the signal contribution corresponding to the best-fit a_τ value ($a_\tau = 0.041$). For comparison, signal contributions with alternative a_τ values are shown as solid red (a_τ =006) or dashed blue (a_τ= 0.04) lines. The bottom panel shows the ratio of the data to post-fit predictions. Vertical bars denote uncertainties from the finite number of data events. Hatched bands represent $\pm 1\sigma$ systematic uncertainties of the prediction with the constraints from the fit applied [6].

of the measurement of the process $\gamma\gamma \to \tau\tau$ is beyond 5 standard deviations. After the fit, the photon-flux uncertainty becomes subdominant and the luminosity uncertainty becomes negligible relative to other sources. The leading contributions to the total systematic uncertainty are: the estimation of the muon trigger efficiency, the τ-lepton decay modelling and the track reconstruction efficiency.

5 Signal strength and constraints on a_τ

The signal strength $\mu_{\tau\tau}$, defined as the ratio of the observed signal yield to the SM expectation assuming the SM value for a_τ , is measured to be: $\mu_{\tau\tau}$= 1.03 $^{+0.06}_{-0.05}$(tot) = 1.03$^{+0.05}_{-0.05}$(stat) $^{+0.03}_{-0.03}$(sys), largely dominated by the limited statistics. A total of 14 templates for different τ values are created to model the dependence of the $\mu - p_T$ distribution on a_τ in the three SRs. The combined-fit value of a_τ is a_τ = 0.041, with the corresponding 68% CL and 95% CL intervals being(-0.050,-0.029) and (-0.057, 0.024), respectively. The higher-than-expected observed yields lead to the highly asymmetric 95% CL interval. This arises from the nearly quadratic signal cross-section dependence on a_τ, caused by the interference of the SM and BSM amplitudes. The expected 95% CL interval is $-0.039 < a_\tau < 0.020$. The impact of systematic uncertainties on the final results is small relative to statistical uncertainties. Figure 10

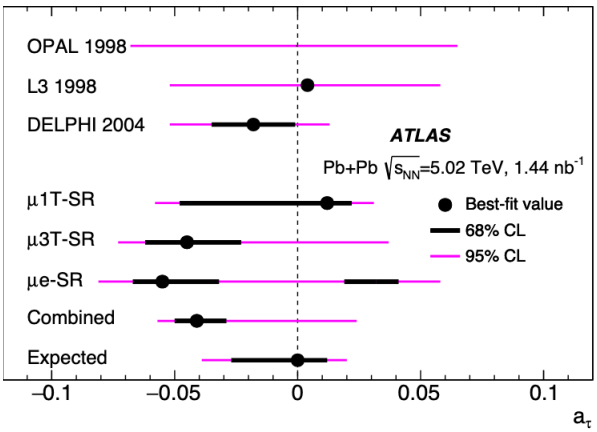

Figure 10. Measurements of a_τ from fits to individual signal regions (including the dimuon control region), and from the combined fit. These are compared with existing measurements from the OPAL, L3 and DELPHI experiments at LEP. A point denotes the best-fit a_τ value for each measurement if available, while thick black (thin magenta) lines show 68% CL (95% CL) intervals. The expected interval from the ATLAS combined fit is also shown [6].

shows the a_τ measurement alongside previous results obtained at LEP. The precision of this measurement is similar to the most precise single-experiment measurement by the DELPHI Collaboration.

6 Conclusions

In summary, τ-lepton pair production in ultraperipheral heavy-ion collisions, $Pb + Pb \rightarrow Pb(\gamma\gamma \rightarrow \tau\tau)Pb$, is observed by ATLAS with a significance exceeding 5 standard deviations in 1.44 nb^{-1} of $\sqrt{s_{NN}}$= 5.02 TeV data at the LHC. The observed event yield is compatible with that expected from the SM prediction within uncertainties. The events are used to set constraints on the a_τ-lepton anomalous magnetic moment, corresponding to $-0.057 < a_\tau < 0.024$ at 95% CL. The precision of the present experiment is limited by the statistical error: there is a large room for significant improvements in run3 and HL-LHC data taking periods.

References

[1] J. Schwinger, Phys. Rev. **73**, 416 (1948).
[2] D. Hanneke, S. Fogwell Hoogerheide and G. Gabrielse, Phys. Rev. A**83**, 052122 (2011).
[3] Muon g-2 collaboration, Phys. Rev. Lett. **126**, 141801 (2021).
[4] The DELPHI Collaboration, Eur. Phys. J. C**35**, 159 (2004).
[5] S. Eidelman and M. Passera, Mod. Phys. Lett. A**22**, 159 (2007).
[6] ATLAS Collaboration, arXiv:2204.13478 [hep-ex], accepted for publication on Phys. Rev. Lett.; https://atlas.web.cern.ch/Atlas/GROUPS/PHYSICS/PAPERS/STDM-2019-19/.
[7] M. Dyndal, M. Klusek-Gawenda, M. Schott and A. Szczurek, Phys. Lett. B **809**, 135682 (2020).
[8] E. Fermi, Z. Phys. **29**, 315 (1924); N. Cimento **2**, 143 (1925).
[9] ATLAS Collaboration, JINST **3**, S08003 (2008).
[10] ATLAS Collaboration, CERN-LHCC-2007-001 (2007); https://cds.cern.ch/record/1009649.
[11] S. R. Klein, J. Nystrand, J. Seger, Y. Gorbunov, and J. Butterworth, Comput. Phys. Commun. **212**, 258 (2017).
[12] N. Davidson, G. Nanava, T. Przedzinski, E. Richter-Was, and Z. Was, Comput. Phys. Commun. **183**, 821 (2012).
[13] G. Avoni et al., JINST **13**, P07017 (2018).